Image Cover Sheet

CLASSIFICATION	SYSTEM NUMBER
UNCLASSIFIED	507274

TITLE

AN EXPERIMENTAL EVALUATION OF SPLIT-BEAM PROCESSING AS A BROADBAND BEARING ESTIMATOR FOR LINE ARRAY SONAR SYSTEM

System Number:

Patron Number:

Requester:

Notes:

DSIS Use only:

Deliver to: FF

An experimental evaluation of split-beam processing as a broadband bearing estimator for line array sonar systems

Stergios Stergiopoulos[a)]
Defence and Civil Institute of Environmental Medicine, P.O. Box 2000, North York, Ontario M3M 3B9, Canada

Anthony T. Ashley
Defence Research Establishment Atlantic, P.O. Box 1012, Dartmouth, Nova Scotia B2Y 3Z7, Canada

(Received 20 May 1996; accepted for publication 3 July 1997)

This paper examines the potential improvements in bearing estimation performance of split-beam processing over full-aperture beamforming for broadband signals. It presents theoretical results in order to define the details of the signal flow in a split-beam processor, and it provides theoretical performance predictions by using Cramer–Rao lower bound (CRLB) analysis. The split-beam processing scheme was implemented in a real-time line array system. Good agreement between the theoretical performance predictions and the associated experimental broadband results were obtained. The experimental results indicate that the advantage of improved bearing estimation performance of the split-beamformer over the conventional full-aperture beamformer may be practically insignificant for passive line array applications because of the split-beamformer's poor performance in detecting very weak broadband signals. © *1997 Acoustical Society of America.* [S0001-4966(97)01311-8]

PACS numbers: 43.60.Gk, 43.30.Wi [JLK]

INTRODUCTION

Sonar array processing includes a large number of algorithms that are quite diverse in concept. However, a common element in most sonar systems is the beamforming process which provides both array gain and target bearing estimation.

Previous theoretical studies[1–4] have addressed two important points regarding the beamforming problem. First, Cramer–Rao lower bound (CRLB) analysis has been used to set an absolute lower bound for the minimum variance achievable by a maximum-likelihood (ML) estimator. Second, CRLB estimates have been used to determine the optimum position configuration for the hydrophones of a line array in order to get optimum estimates for a target's bearing or range or position. When quantifying bearing performance, MacDonald and Schultheiss[1] and Carter[2] have shown that, when placing half the towed array sensors exactly at one end and half exactly at the other end, the theoretical lower limit is achieved indicating optimum array configuration for bearing estimates. However, the above optimum array configuration is useful only under the assumed condition that signal and noise are stationary Gaussian processes embodied in an isovelocity medium. Furthermore, several hydrophone elements could never be physically located at the identical spot on both ends of the line array. In practice, the sensors would be placed at moderate fraction of a half-wavelength spacing. As a result of this kind of practical constraint, it has been shown[1] that a nearly optimal technique for bearing estimation is the *split-beam processing method.*

In split-beam processing a linear array is assumed to consist of two subarrays placed towards each end of a hydrophone array configuration. At each subarray, beams are steered simultaneously in the same direction by means of conventional beamforming. Then, the corresponding output pairs of beam time-series are cross correlated in order to derive time delay measurements for bearing estimates. Theoretically, split-beam processing can provide better broadband bearing resolution than conventionally beamforming the full aperture.[1,4]

Even though the improved bearing estimation performance of the split-beam processing over full aperture beamforming is more pronounced for broadband signals located in the endfire directions of a towed array, this advantage may be practically insignificant for passive towed array applications because of the split-beamformer's poor performance in detecting very weak signals.[2,3,5,13,14] However, despite these performance problems, the split-beamforming concept was considered, until very recently, as an attractive option by the sonar system designers. The reason is that hardware restrictions and computing architecture limitations favored suggestions[2] that included the placing of two or three subarrays widely spaced over a baseline of a fixed length. The aim of this paper is to address these concerns experimentally and to assess their importance with respect to system applications.

The material in Secs. I–III of this paper addresses the theoretical principles[1–5,13–15] to provide the details of an optimum split-beamformer's signal processing flow and to assess its performance. The poor performance of the split-beam processing versus the full-aperture beamforming, predicted in Secs. II and III, is verified experimentally in Sec. IV by (i) implementing the broadband split-beamforming concept in a real-time line array system as shown in Fig. 3, and (ii) comparing the split-beamformer's performance with that of the full-aperture beamformer's output, which is shown in Fig. 11.

[a)]Electronic mail: stergios@dciem.dnd.ca

I. BACKGROUND

Consider a horizontal line array with N omnidirectional hydrophones equally spaced at distance δ in an anisotropic ocean. Furthermore, assume an incoming acoustic signal from a distant source with bearing θ, measured from the broadside direction of the line array. The signal is sampled at time increment Δt with $t_i = i\Delta t$, where $i = 1,2,...,K$, K being the number of data samples for each one of the hydrophone time series. The time series are expressed by

$$x_n(t_i) = s(t_i + n\tau) + \varepsilon_{n,i}(0,\sigma_\varepsilon), \tag{1}$$

where $n = 0,1,...,N-1$, N is the number of hydrophones and τ is the time delay between two successive hydrophones of the signal wavefront arrival. Here $X_n(f) = \Sigma_{i=1}^{K} x_n(t_i) \times \exp(-j2\pi f t_i)$ is the Fourier transform of $x_n(t_i)$ at frequency f, $c = f\lambda$ is the speed of sound in the ocean, and λ is the wavelength; $\varepsilon_{n,i}(0,\sigma_\varepsilon)$ are independent, zero mean, Gaussian random variables with standard deviation σ_ε.

Quantitative estimates of the spatial coherence for signals from a line array are provided by the cross-spectral density matrix between any set (n,m) of two hydrophone time series of the line array with spatial separation $\delta_{nm} = (n-m)\delta$. An estimate of the cross-spectral density matrix[2,3] in the frequency domain is given by

$$R_{nm}(f,\delta_{nm}) = E[X_n(f)X_m^*(f)], \tag{2}$$

where $E[\cdots]$ denotes the expectation operator and * denotes complex conjugate. The above space-frequency correlation function can be related to the angular power directivity pattern of the source, $\Psi_s(f,\theta)$, via a Fourier transformation[6] by using a generalization of Bello's concept[7] of time-frequency correlation function $[t \Leftrightarrow 2\pi f]$ into space $[\delta_{nm} \Leftrightarrow 2\pi f \sin\theta/c]$. The correlation function, $R_{nm}(f,\delta_{nm})$, has numerous uses in other areas such as time delay estimation, beamforming, and determination of array gain.

Previous studies[8] have shown that for a signal embedded in a spatially white noise field, the *conventional beamformer* (CBF) without shading is an optimum beamformer for bearing estimation and its variance achieves the theoretical CRLB bound. When there are multiple signals, however, the deterioration of performance for the CBF is well-known and well documented with defects of "spatial beam leakage" and degradation in spatial resolution.[16] The narrow-band CBF is defined by $B(f,\theta_s) = D^*(f,\theta_s)X(f)$, where the nth element of the steering vector $D(f,\theta_s)$ is

$$\eta_n(f,\theta_s) = \exp[j2\pi f \delta_{1n} \sin\theta_s/c]$$

and $X(f)$ is an N-dimensional vector of hydrophone data $X_n(f)$ at frequency f. The term $\tau_s = \delta_{1n}\sin\theta_s/c$, in the steering vector $\eta_n(f,\theta_s)$, represents the time delay between the first and nth hydrophones of the array for an incoming plane wave with direction of propagation θ_s.

Cross correlation of the corresponding pairs of beam time series in split-beam processing is the main processing step to provide time delay estimates τ_s, which can be interpreted as bearing angles θ_s expressed by

$$\theta_s = \cos^{-1}(c\tau_s/\Delta L), \tag{3}$$

where ΔL is the distance between the two acoustic subarray centers. A tutorial review on time delay estimation is provided by Carter.[2–4] Practical issues of robustness for cross-correlation processing are also discussed by Ferguson.[5]

For bandwidth-limited signals the cross-correlation output of the split-beam processing is a cosine function modulated by a sinc function [see Eq. (5)], therefore the time spreading increases as the bandwidth decreases. As the signal bandwidth becomes a small fraction of the center frequency, then the time delay estimate from the cross-correlator's output becomes more ambiguous.[13,14] For temporally white noise the cross-correlation output $R_\theta(\tau)$ of the corresponding pairs of beam time series in split-beamforming is expressed by

$$R_\theta(\tau) \propto \delta(\tau), \tag{4}$$

for bandwidth limited signals is expressed by

$$R_\theta(\tau) = B_w\left[\frac{\sin(\pi B_w \tau)}{\pi B_w \tau}\right]\cos(2\pi f_0 \tau), \tag{5}$$

where B_w is the bandwidth of the signal and $0 < f_0 - (B_w/2) \leqslant f \leqslant f_0 + (B_w/2)$, and for a monochromatic signal is expressed by

$$R_\theta(\tau) \propto \cos(2\pi f_0 \tau). \tag{6}$$

Furthermore, for signals close to broadside ($\theta_s = 0$) the resolution properties of the split-beamformer are governed by the width of the main lobe of the correlator's output. Thus, for two detected signals with bearings θ_1 and θ_2 the corresponding time delay estimates, τ_1 and τ_2, provided at the output of the split beamformer, will be resolvable if their difference satisfies the relation

$$\tau_2 - \tau_1 = \frac{\Delta L}{c}(\cos\theta_2 - \cos\theta_1) \geqslant \frac{\mu}{B_w}, \tag{7}$$

where μ is a constant that depends on the definition of resolution. Assume for simplicity ($\theta_1 = 0$, i.e., broadside) then $\cos\theta_2 = \mu c/(B_w \Delta L)$ or, more general,

$$\theta = \cos^{-1}\left(\frac{\mu c}{B_w \Delta L}\right), \tag{8}$$

which is Eq. (3) with $\tau_s = \mu/B_w$. Based on Eq. (8) and for $\mu = 1$, which assumes ideal bandpass signals, numerical results in Figs. 1 and 2 illustrate the effects of the signal bandwidth and the subaperture separation ΔL on the effective angular resolution performance of the split-beamformer. In particular, Fig. 1 plots for two cases of subaperture separation, ΔL, the angular resolution performance of a split beamformer as a function of the signal's bandwidth, B_w. Figure 2 shows the effects of subaperture separation, ΔL, on the minimum signal bandwidth, B_w, which is required to achieve the indicated angular resolution.

II. SIGNAL PROCESSING FLOW FOR A SPLIT-BEAMFORMER

Before we present the signal processing flow of a split beamformer implemented in a real-time line array system, it is important to discuss briefly prefiltering operations that im-

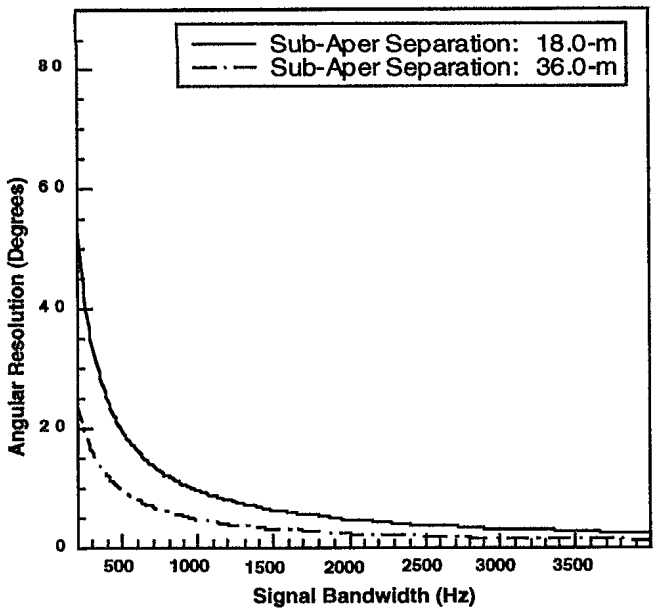

FIG. 1. Effects of signal bandwidth versus angular resolution for a split-beamforming process. Two cases have been considered having subaperture separation of 18 m (shown by the solid line) and 36 m (shown by the dashed line).

prove the cross-correlation processing performance and, as a result, the time delay and bearing estimation process associated with split-beam processing.

Improvements in the time delay estimation process can be obtained through the application of various prefilters in order to accentuate the signal passed to the correlator at those frequencies at which the SNR is highest.[4] In other words, the highest weighting will be applied to cross-spectral estimates with the least variance in the phase error estimates. The same type of prefiltering is provided by the generalized Eckart filter,[15] which maximizes the SNR of the correlator output. In practice, however, the Eckart filter requires knowledge or estimation of the signal and noise spectra.

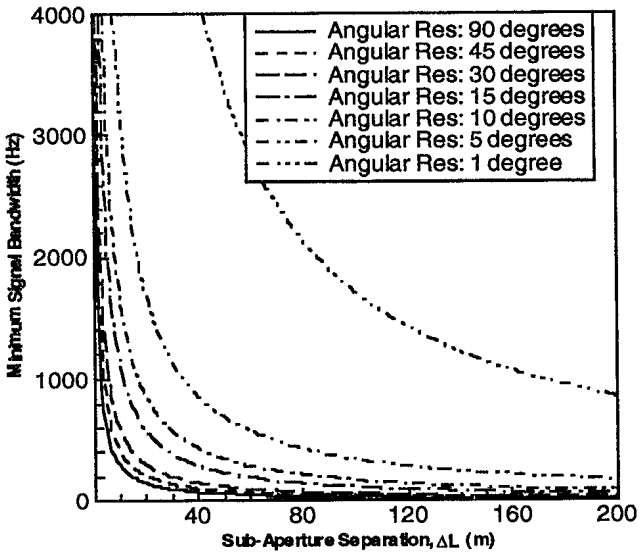

FIG. 2. Effects of subaperture separation and signal bandwidth on selected cases of angular resolution performance by a split-beamforming process.

In the time domain, prefiltering includes the application of filters to the two time series prior to their cross-correlation, while in the frequency domain, prefiltering includes the application of windows or weighting functions to the cross-spectral density function before the inverse FFT process. Therefore, if $R_{nm}(f,\delta_{nm})$ is the correlation output in the frequency domain between two hydrophone time series with δ_{nm} being the hydrophone separation, f is in the frequency range of $0<f_0-(B_w/2)\leqslant f\leqslant f_0+(B_w/2)$, B_w is the signal bandwidth, and f_0 is the center frequency, then the prefiltered cross-correlation output is

$$R_{\theta_s}(f)=W(f)\times R_{nm}(f,\delta_{nm}), \tag{9}$$

where $W(f)$ is a filter defined below by Eq. (10). The inverse FFT of $R_{\theta_s}(f)$ provides the cross-correlation time series $r_{\theta_s}(\tau)$. Since estimates of $W(f)$ are a function of the signal and noise spectra, the signal's coherence properties must be either known *a priori* or estimated. Ferguson[5] has examined experimentally the performance characteristics of three different filters and has discussed practical aspects associated with this kind of prefiltering process. One of the above three prefilters is the *phase transform* processor,[4] which is an *ad hoc* technique that uses only the cross-spectral phase information and it is defined by

$$W(f)=|R_{nm}(f,d_{nm})|^{-1/2}. \tag{10}$$

The Eckart filter[15] unlike the phase transform processor attaches zero weight, $W(f)=0$, to bands where $R_{nm}(f,d_{nm})=0$. However, the Eckart filter requires knowledge or estimation of the signal and noise characteristics to be integrated in the signal processing flow of a real time split-beam processor, which is a very difficult requirement to fulfill. For the present real time system application, we have chosen to use the *phase transform* as a filter, because it does not require knowledge or estimation of the shape of the signal and noise spectra.

Shown in Fig. 3 is the processing configuration of split-beam processing for a line array system. At each subarray, beams are steered simultaneously in the same direction by means of frequency domain conventional beamforming without spatial shading. The frequency domain beamforming outputs are made equivalent to the FFT of the time domain beamformers' outputs by applying proper selection of beamforming weights and careful data partitioning. This equivalence corresponds to implementing FIR filters via circular convolution.[9]

Then, the corresponding output pairs of frequency domain beams $[B^F(f,\theta_s)$ and $B^A(f,\theta_s)]$ are cross correlated to form the beam cross spectra, $\Phi(f,\theta_s)=B^F(f,\theta_s)\times B^{A*}(f,\theta_s)$, for all the frequency bins of the signal's bandwidth B_w, where $0<f_0-(B_w/2)\leqslant f\leqslant f_0+(B_w/2)$. Prefiltering is applied next by weighting the terms $\Phi(f,\theta_s)$ by the phase transform $W(f)=|\Phi(f,\theta_s)|^{-1/2}$. The inverse FFT of $\{W(f)\times\Phi(f,\theta_s)\}$ provides a cross-correlation time series for each beam steered at θ_s. The peaks associated with the cross-correlation outputs provide differential time delay estimates and, as a result, bearing estimates according to Eq. (3). Integration of the bearing estimates from all the cross-

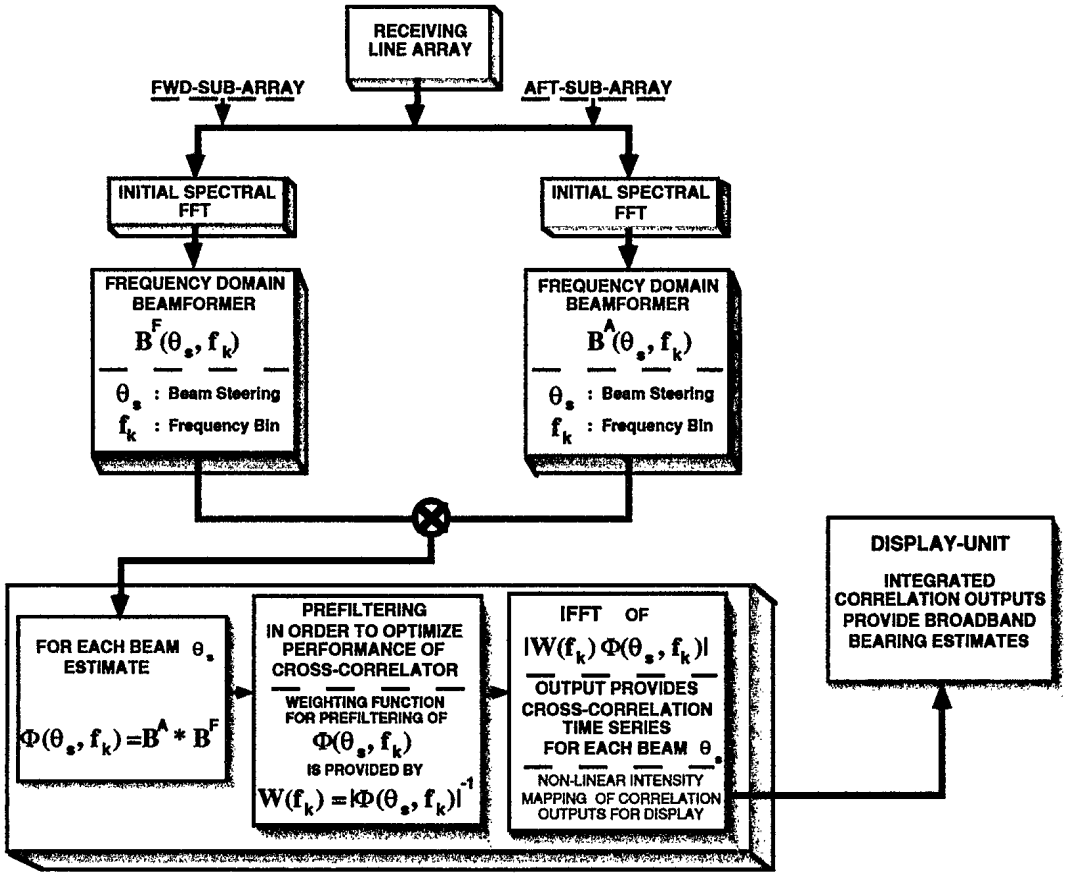

FIG. 3. Signal processing flow of a split-beamformer implemented in a real time system.

correlated beams and their display as a function of time produces the main output of the split-beamformer.

III. THRESHOLD EFFECTS

In this section, the CRLB analysis and computer simulations are used to define and compare quantitatively the performance of the split-beamformer (defined in Sec. II) versus the full aperture beamformer.

Typically, the performance of an unbiased estimator is represented as the variance in the estimated parameters. If the *a priori* probability of detection is close to unity, the minimum variance achievable by any unbiased estimator is provided by the *Cramer–Rao Lower Bound* (CRLB).[10,11] In this case, if there exists a signal processor to achieve the CRLB, it will be the maximum-likelihood estimation (MLE) technique. The above requirement associated with the *a priori* probability of detection is essential because if it is less than one, then the estimation is biased and the theoretical CRLBs do not apply.[10] This general framework of optimality is essential in order to account for Middleton's (Ref. 10, p. 787) warning that a system optimized for the one function (detection or estimation) may not be necessarily optimized for the other.

Let θ_i denote the *maximum likelihood estimate* (MLE) of the parameter of interest and $\sigma^2_{\theta_i}$ denote the variance of the estimate $\widetilde{\theta}_i$ for the parameter θ_i that is described by a model, such as the one in Eq. (1). The Cramer–Rao[10,11] bound states that the variance $\sigma^2_{\theta_i}$ of the best unbiased estimate $\widetilde{\theta}_i$ of the parameter of θ_i has a CRLB, which is given by the diagonal elements of the Fisher information matrix.[10,11] This CRLB is used as a standard of performance and provides a good measure for the performance of a signal processing algorithm. Furthermore, for each estimator it is well known that there is a range of *Signal-to-Noise Ratio* (SNR) in which the variance of the estimates rises rapidly as SNR decreases. This effect, which is called the *threshold effect of the estimator*, determines the range of SNR of the received signals for which the parameter estimates can be accepted. Thus, estimation of the threshold effect is essential in the selection of practical robust sonar signal processing.

At this point it is important to note that the CRLB applies to small or local errors only, hence it is not useful below threshold where large errors occur. Other bounds are thus needed to characterize the large error region. One such bound is the Zik–Zakai lower bound (ZZLB).[13,14]

In this study, the CRLB analysis and computer simulations have been used to define and compare quantitatively the performance of the split-beam processing for different cases of effective signal bandwidth and subaperture separation. Shown by the three curves in Fig. 4 are the theoretical CRLB, $\sigma^2_{\theta_{\mathrm{CRLB}}}$ for the bearing as a function of SNR for the case of one source. These theoretical CRLB estimates were derived from MacDonald and Schultheiss [Ref. 1, Eq. (20)] and are for a split-beam processor including two subaper-

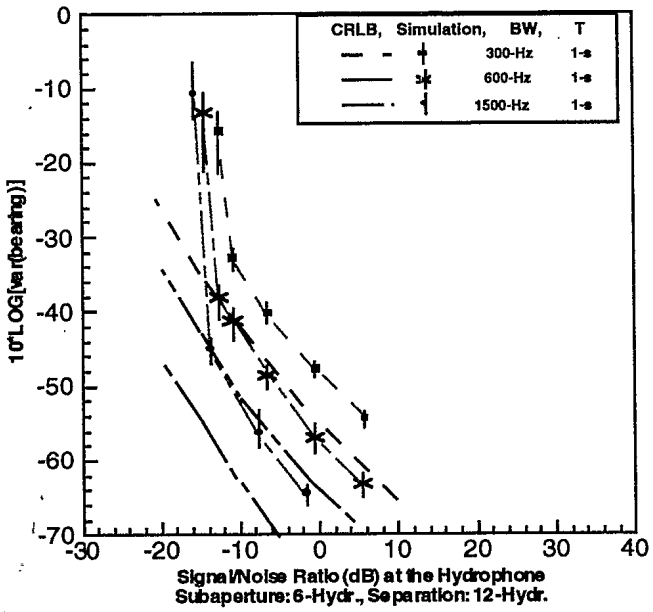

FIG. 4. Performance analysis of a split-beamformer for three different cases of effective signal bandwidth. Curves show the corresponding theoretical CRLB estimates.

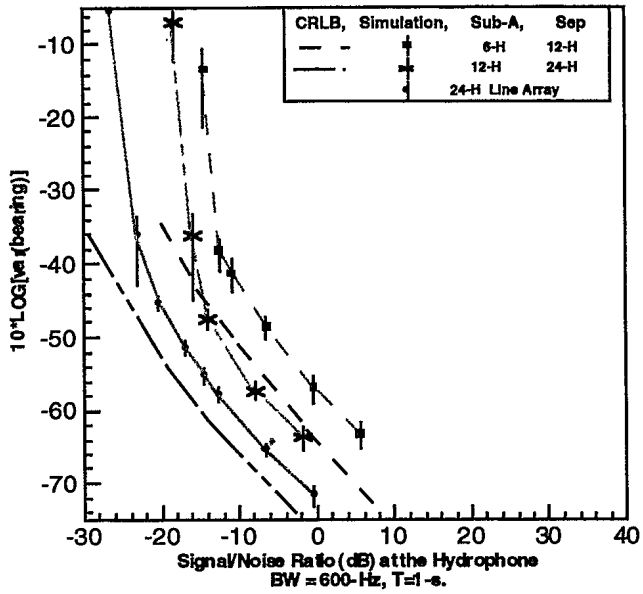

FIG. 6. Performance analysis of a split-beamformer for two different cases of subaperture sizes and for a full aperture beamformer. The signal bandwidth was 600 Hz and the observation period was 1 s. Curves show the theoretical CRLB estimates.

tures each having 6 hydrophones. The separation between the two subapertures is 12 hydrophone spacings as this is illustrated in Fig. 5. Moreover, the geometric configuration of the above figure shows the concept of this study of forming the two subapertures at both ends of an equi-spaced line array. For the above three CRLB estimates, $\sigma^2_{\theta_{\text{CRLB}}}$, the corresponding signal bandwidths are 300, 600, 1500 Hz; and for all of them the processing period was the same and equal to 1 s.

For the same signal bandwidths and subaperture configuration, computer simulations were also considered for the calculation of the variance $\sigma^2_{\theta_s}$ of bearing estimates. Figure 4 presents the estimates of $\sigma^2_{\theta_s}$ derived by a split-beam processor with a signal processing flow, which is shown in Fig. 3. The ocean model for the simulations is a direct path isovelocity environment.

In Fig. 4, the difference between the theoretical CRLB estimates, $\sigma^2_{\theta_{\text{CRLB}}}$ and the simulations, $\sigma^2_{\theta_s}$ is approximately 7.8 dB and agrees with predictions discussed in Ref. 1, Eq. (35). It is apparent by the above results that the performance of the split-beamformer improves as the signal bandwidth increases. The threshold effect is also shown by the rapid rise of the variance of the bearing estimates for SNR values in the range of -12 dB at the hydrophone.

The results depicted in Fig. 6, from the same kind of computer simulations as those of Fig. 4, show how bearing variance depends upon aperture size. The curves in Fig. 6 provide the theoretical CRLB, $\sigma^2_{\theta_{\text{CRLB}}}$, [Ref. 1, Eqs. (19), (20)] for the bearing as a function of SNR for the case of one source with effective signal bandwidth of 600 Hz. These theoretical CRLB estimates are for two different kinds of subaperture configurations, shown in Fig. 6. Results indicated by solid circles are from computer simulations derived by full aperture beamforming a 24-hydrophone line array. The processing period for this signal was equal to 1 s. In this case of full aperture beamforming, the threshold effect is shown to be in the range of -22 dB at the hydrophone. Solid squares in the same figure present the variance estimates $\sigma^2_{\theta_s}$ for the same 600-Hz signal bandwidth and 1-s integration period. These estimates were derived by applying split-beam processing on two subarrays of 6 hydrophones each and separated by 12 hydrophones. The threshold effect of the split-beam processing is in the range of -12 dB at the hydrophone.

In order to quantify the effects of larger subapertures, this split-beamforming analysis was also applied to the same signal and for subarrays of 12 hydrophones each and separated by 24 hydrophones for an extended array. The simulation results of $\sigma^2_{\theta_s}$, in this case, are shown by the star symbols in Fig. 6 and indicate inferior performance than that of the fully populated 24-hydrophone array, shown by the solid circles in the same figure. In the simulation, the conventional beamformer included uniform spatial shading across the hydrophone samples. Thus, although the two subarrays of 12 hydrophones each have in total the same number of hydro-

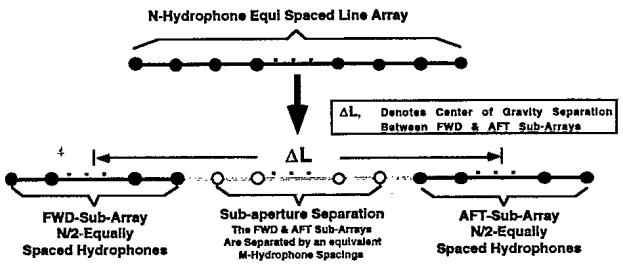

FIG. 5. Geometric configuration showing the concept of this study of forming the two sub-apertures at both ends of an equi-spaced line array.

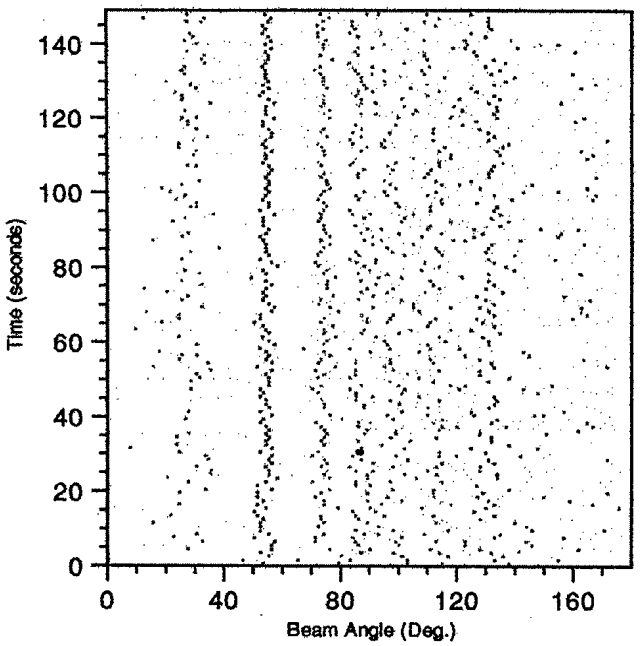

FIG. 7. Bearing estimates as a function of time from real sea data and for a split-beam processing scheme shown in Fig. 3. The signal bandwidth was 200 Hz and the coherent processing period was 1 s. The two subapertures (with size of 6 hydrophones each) were separated by 12 hydrophone spacings.

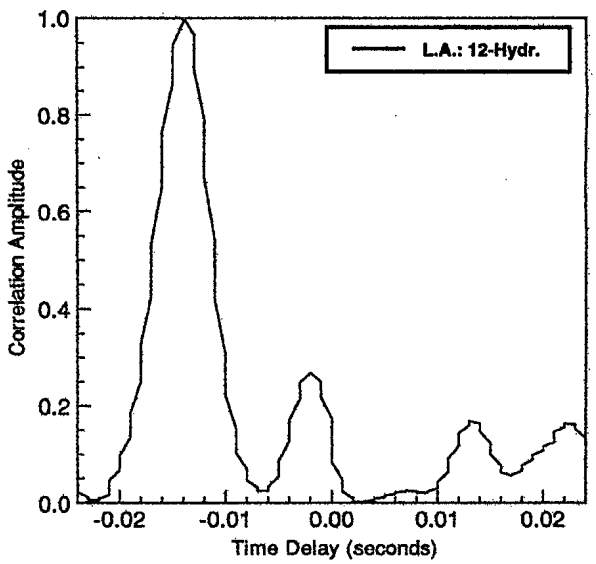

FIG. 8. Cross-correlation output from the corresponding pair of subaperture beams steered simultaneously in the same direction of 60°. The cross-correlation peaks in this figure indicate the differential time delays that provide the associated bearing estimates shown in the previous Fig. 7.

phones as the 24-hydrophone fully populated array, the threshold value of the split-beam processing is worse than that of the full aperture beamformer.

IV. REAL EXPERIMENTAL RESULTS

The set of experimental data of this study represents an acoustic field consisting of radiated noise including strong narrowband and broadband features from distant ships and geological equipment in acoustic conditions typical of a North Atlantic sea state 4. The data were collected over 150 s on a 24 hydrophone line array with 2-m spacing. The velocity profile was a typical North Atlantic summer ocean environment.

The subaperture configuration for split-beam processing included two subarrays with 6 hydrophones each at both ends of the deployed array and separated by 12 hydrophones spacing. Application of the split-beam processing scheme on the above subarray configuration provided broadband bearing results shown in the following figures. The length of the processed time series was 1 s and the signal bandwidth was 200 Hz. Figure 7 shows the bearing estimates as a function of time provided by the output of the split-beamformer of Fig. 3, which utilizes prefiltering. In Fig. 8 the cross-correlation output is presented from one snapshot of the corresponding pairs of beams steered simultaneously in the same direction of 60°, with respect to the line array axis, where a loud broadband target was known to exist. The cross-correlation peaks in this figure indicate the differential time delays, which provide the associated bearing estimates according to Eq. (6).

In order to illustrate the influence of the prefiltering process on the performance of the split-beamformer, the weighting coefficients $W(f)$ of the prefilter were set to unity. That is prefiltering was "off." In this case, split-beam processing of the same data set of Fig. 8 provided poor bearing results which are shown in Fig. 9. Another way to demonstrate the relative performance of the prefiltering process is to examine the corresponding cross-correlation output from one snapshot of the corresponding pairs of beams steered simultaneously in the same direction of 60°, as those of Fig. 8. The associated cross-correlation output, for split-beam processing

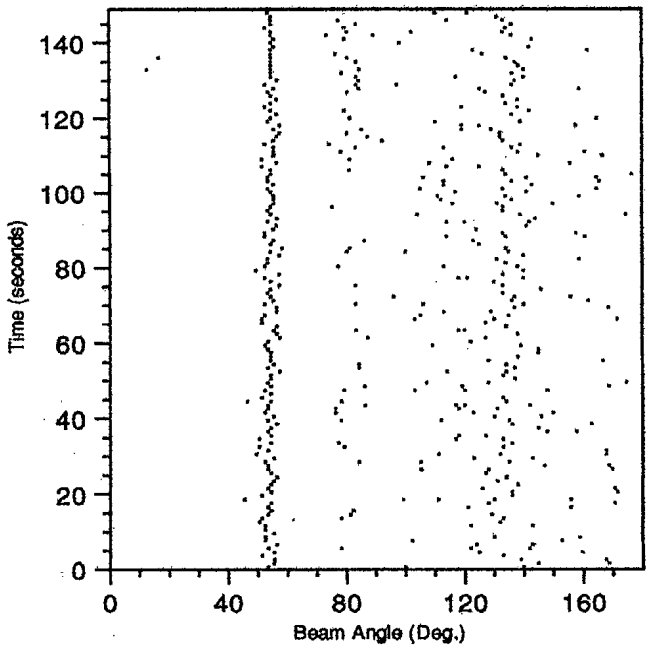

FIG. 9. Bearing estimates as a function of time for a split-beam processing scheme shown schematically in Fig. 3. In this case the weighting coefficients $W(f)$ of the prefilter were set to unity. The pronounced difference in performance between the results of this figure with those of Fig. 7 indicates the necessity to include the prefiltering process in the split-beamformer.

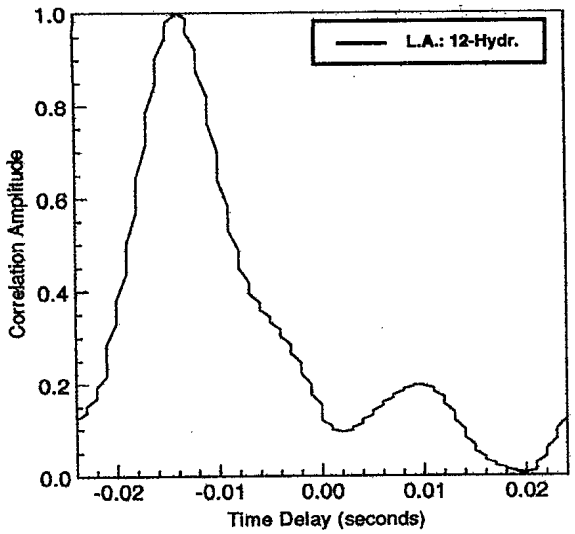

FIG. 10. Cross-correlation output from the corresponding pair of subaperture beams steered simultaneously in the same direction of 60°. In this case the weighting coefficients $W(f)$ of the prefilter were set to unity. The cross correlation peaks in this figure indicate the differential time delays that provide the associated bearing estimates shown in the previous Fig. 9.

with prefilter weighting coefficients set to unity, is shown in Fig. 10. This figure shows fewer correlations peaks (or targets) than the results of Fig. 8.

The correlation peaks in Figs. 7–10 refer to distant multiple targets and their associated multipath characteristics.

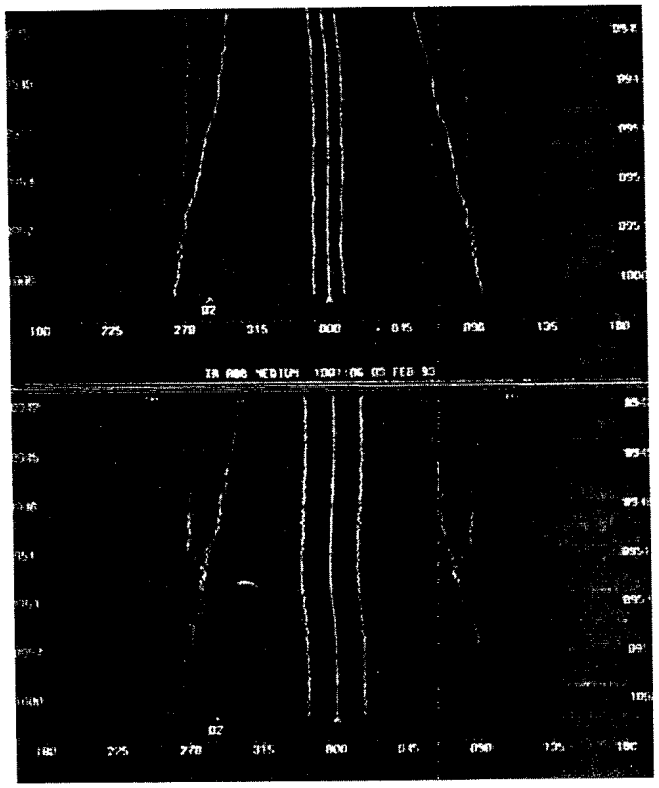

FIG. 11. Bearing estimates as a function of time from real line array data, including both split-beam and full-aperture conventional beamforming processing schemes under a parallel configuration. The upper part shows the bearing estimates from a full-aperture conventional beamformer and the lower part from the corresponding split-beamformer.

Since Figs. 8 and 10 refer to the same set of real data, their pronounced difference indicates the necessity to include the prefiltering process in split-beam processing. Furthermore, the above real data results confirm theoretical predictions on prefiltering process, which are discussed in Refs. 1–4.

Figure 11 shows broadband bearing results from a split-beam and a full aperture conventional beamformer implemented for a real experimental array system. The array configuration was as described above. The upper part of this figure shows broadband bearing results derived by beamforming all 24 hydrophones of the array. The lower part in the same figure shows the broadband bearing estimates provided by the output of the split-beamformer. Both the split-beam and full aperture beamforming operations were applied simultaneously on the same set of data. The middle solid line in both displays shows the heading of the tow ship. The two almost vertical traces, which appear to be parallel with the heading of the tow ship, are the bearing estimates of the tow vessel detected at the forward endfire of the towed array.

Differences in the bearing estimates of the tow vessel between the upper and lower displays indicate the superior performance of the split beam processor to provide better accuracy in bearing estimates at the endfire beams of the towed array than that of the full aperture conventional beamformer. This confirms predictions[1–4] that the bearing estimates located at the endfire of the towed array are biased when are provided by the full aperture beamformer. In fact this was the main argument and driving force to pursue this implementation study. The objective was to quantify experimentally that the split-beam processor provides significant angular resolution improvement over that of the full aperture beamformer for targets located at the endfire beams of a towed array.

In conclusion, the results in Fig. 11 are in agreement with those of Figs. 4 and 6, which predicted the characteristics and the performance difference between the full and subaperture beamforming. As discussed in Sec. III, a dramatic performance difference associated with the detection of weak signals should be expected to be in favor of the full aperture beamforming over the split-beam processing. This prediction has been confirmed by the results of Fig. 11. The only advantage that the split-beam processing has with respect to the full aperture beamforming is a better angular resolution performance at the end-fire beams, which is restricted only for cases with very strong signals.[1–4]

V. CONCLUSION

In conclusion, this study has shown that the improved bearing estimation performance of the split-beam processing over the full aperture beamforming is practically insignificant for passive line arrays because of the split-beamformer's poor performance in detecting very weak signals.

Furthermore, in practical sonar applications the acoustic signals of interest are embedded in spatially and temporally partially correlated noise fields, which is in sharp contrast with the assumption of this study that the noise field is spatially and temporally white. The general case of broadband and narrowband signals embedded in a spatially and temporally anisotropic noise field requires that the spatial filtering

operation for optimum detection should include adaptation of the sonar signal processing according to the noise characteristics. This last argument suggests a need for adaptive beamforming in sonar systems.

In summary, the results of this experimental study verify that the theoretical developments play an important role in assisting the sonar system designers to define optimum signal processing concepts and in predicting the performance of a sonar line array system incorporating split-beamformers.

[1] V. H. MacDonald and P. M. Schulteiss, "Optimum passive bearing estimation in a spatially incoherent noise environment," J. Acoust. Soc. Am. **46**, 37–43 (1969).

[2] G. C. Carter, "Coherence and Time Delay Estimation," Proc. IEEE **75**(2), 236–255 (1987).

[3] G. C. Carter and E. R. Robinson, "Ocean Effects on Time Delay Estimation Requiring Adaptation," IEEE J. Ocean Eng. **18**, 367–378 (1993).

[4] C. H. Knapp and G. C. Carter, "The generalized correlation method for estimation of time delay," IEEE Trans. Acoust. Speech Signal Process. **ASSP-24**, 320–327 (1976).

[5] B. G. Ferguson, "Improved time-delay estimates of underwater acoustic signals using beamforming and prefiltering techniques," IEEE J. Ocean Eng. **14**(3), 238–244 (1989).

[6] S. Stergiopoulos, "Limitations on towed-array gain imposed by a non isotropic ocean," J. Acoust. Soc. Am. **90**, 3161–3172 (1991).

[7] P. A. Bello, "Characterization of randomly time-variant linear channels," IEEE Trans. Commun. Syst. **10**, 360–393 (1963).

[8] W. M. X. Zimmer, "High resolution beamforming techniques, performance analysis," SACLANTCEN SR-104, La Spezia, Italy, SACLANT Undersea Research Centre (1986).

[9] A. Mohammed, "A high-resolution spectral analysis technique," DREA Memorandum 83/D, Defence Research Establishment Atlantic, Dartmouth, N.S., Canada (1983).

[10] D. Middleton, *Introduction to Statistical Communication Theory* (McGraw-Hill, New York, 1960), p. 787.

[11] H. L. Van Trees, *Detection, Estimation and Modulation Theory* (Wiley, New York, 1968).

[12] S. Stergiopoulos and A. T. Ashley, "Editorial," Special issue on Sonar System Technology, IEEE J. Ocean Eng. **18**(4), 361–366 (1993).

[13] J. P. Ianniello, "Lower Bounds on Worst Case Probability of Large Error for Two Channel Time Delay Estimation," Trans. Acoust. Speech Signal Process. **ASSP-33**(4), 1102–1110 (1985).

[14] J. Ziv and M. Zakai, "Some Lower Bounds on Signal Parameter Estimation," IEEE Trans. Inf. Theory **IT-15**, 386–391 (1969).

[15] C. Eckart, "Optimal Rectifier Systems for the Detection of Steady Signals," Univ. California, Scripps Inst. Oceanography, Marine Physical Lab., Rep. SIO 12692, SIO Ref. 52-11, 1952.

[16] S. Haykin, *Advances in Spectrum Analysis and Array Processing* (Prentice-Hall, Englewood Cliffs, NJ, 1991).